



# Comparison of Reactive Blue 203 Dye Removal Using Ultraviolet Irradiation, Ferrate (VI) Oxidation Process and MgO Nanoparticles

Amirreza Talaiekhozani<sup>1,2</sup>, Nilofar Torkan<sup>3</sup>, Fahad Banisharif<sup>4,5</sup>, Zeinab Eskandari<sup>3</sup>, Shahabaldin Rezania<sup>6</sup>, Junboum Park<sup>6</sup>, Farham Aminsharei<sup>7,8</sup>, Ali Mohammad Amani<sup>2,9</sup>

<sup>1</sup>Department of Civil Engineering, Jami Institute of Technology, Isfahan, Iran

<sup>2</sup>Biophotonics Research Center, Shiraz University of Medical Sciences, Shiraz, Iran

<sup>3</sup>Department of Chemical Engineering, Jami Institute of Technology, Isfahan, Iran

<sup>4</sup>Chemical Engineering Department, Faculty of Petroleum and Gas Engineering, Iran University of Science and Technology, Tehran, Iran

<sup>5</sup>R&D Department, NirouChlor, Isfahan, Iran

<sup>6</sup>Department of Civil and Environmental Engineering, Seoul National University, Seoul, Republic of Korea

<sup>7</sup>Department of Safety, Health and Environment, Najafabad Branch, Islamic Azad University, Najafabad, Iran

<sup>8</sup>Human Environment and Sustainable Development Research Center, Najafabad Branch, Islamic Azad University, Najafabad, Iran

<sup>9</sup>Department of Medical Nanotechnology, Shiraz University of Medical Sciences, Shiraz, Iran

## \*Correspondence to

Amirreza Talaiekhozani,

Email: amirtkh@yahoo.com,  
atalaie@jami.ac.ir

Published online December  
29, 2018

## Abstract

This study investigated the effect of various parameters on the removal of Reactive Blue 203 dye from wastewater using ferrate(VI) oxidation process, ultraviolet radiation (UV) radiation and MgO nanoparticles under batch mode. Although several studies have been carried out on dye removal, there is no study on the removal of Reactive Blue 203 dye using ferrate(VI) oxidation process, UV radiation, and MgO nanoparticles. Therefore, the aim of this study is to investigate the effect of different factors including pH, temperature, contact time, the intensity of UV radiation and the concentration of MgO nanoparticles on Reactive Blue 203 dye removal using the above-mentioned methods. The results showed that the best pH values for dye removal using UV radiation, ferrate(VI), and MgO nanoparticles were 13, 1 and 13, respectively. The best temperature for Reactive Blue 203 dye removal using ferrate(VI) was 50°C. Hence, temperature variation had no significant effect on Reactive Blue 203 dye removal using UV irradiation and absorption by MgO nanoparticles. Based on the results, the best contact time was 15 minutes using UV radiation. The removal of Reactive Blue 203 dye using ferrate(VI) oxidation process was a quick reaction, and in a fraction of a second, the reactions were completed. The results showed that dye removal using MgO nanoparticles could be described by the Temkin isotherm. Therefore, the contact time was not considered as an effective parameter. In addition, the maximum dye removals were 95, 85 and 94% using UV irradiation, ferrate(VI) and MgO nanoparticles.

**Keywords:** Ferrate(VI), MgO nanoparticles, Ultraviolet radiation, Wastewater treatment, Reactive Blue 203 dye

Received September 11, 2018; Revised November 20, 2018; Accepted December 6, 2018

## 1. Introduction

Nowadays, environmental issues such as waste pollution have become a global concern. Therefore, effective wastewater treatment is one of the world's challenges (1). Dyes are one of the most important pollutants in wastewater (2). Dyes are used in a wide range of industries, including textile factories. Generally, the wastewater released from the textile industry has a high level of biological oxygen demand (BOD), chemical oxygen demand (COD), dye and dissolved solids. Jorfi et al reported that thousands

of tons of dyes are used in textile industries annually and 10% of them are released into the environment (3). Textile wastewater contains various types of synthetic dyes such as Azo compounds, which are highly soluble, stable and inexpensive (4). Discharging dyes causes many environmental problems. For example, dyes increase the BOD of water resources as the aerobic bacteria use dyes as a source of carbon and energy. In addition, dyes prevent sunlight from penetrating to water (5, 6). Therefore, the life of many plants and microorganisms is threatened

by dyes in contaminated water (7). Azo dyes such as Reactive Blue 203, Blue 19, Reactive Red 198 and Acid Red 52 dye, are toxic, carcinogenic and contain mutagenic compounds (8,9). These dyes can be categorized as recalcitrant compounds and threaten human and animal health. Reactive Blue 203 dye is a hazardous compound, which is widely used and found in large amounts of textile wastewater (10). The molecular structure of the Reactive Blue 203 dye is shown in Figure 1.

As the dye removal from wastewater using conventional methods such as screening, settling, coagulation, and flocculation is not effective, finding a suitable and effective method is vital. Disinfection is the last part of a wastewater treatment system and chlorine is the most commonly used disinfectant in such systems. Once chlorine is added to wastewater, a reaction starts and results in dye oxidation (11). In this reaction, small amounts of trihalomethanes are produced, which are the most important chlorination byproducts (12). Some types of trihalomethanes, such as chloroform, cause cancer in animals and may have long-term adverse effects on human health, including liver cancer (13). These reasons demonstrate the importance of removing various dyes from textile wastewater.

Many researchers have studied various methods of dye removal from wastewater such as biological processes, advanced oxidation processes and absorption processes (14-17). Recently, Rai et al found that ferrate(VI) has coagulant properties during the oxidation of various contaminants in wastewater under different conditions (18). Ferrate(VI) is the most powerful oxidizing agent ever known when it is used in an acidic condition (19). Studies showed that no harmful by-products are generated during oxidation of organic pollutants including dyes in wastewater using ferrate(VI) (20). Ferrate(VI) is gradually converted to ferric(III) which is a well-known coagulant. Ferrate(VI) is able to kill microorganisms and it may be considered as a suitable alternative to chlorine (19). Therefore, oxidation, coagulation, and disinfection can happen when ferrate(VI) is used for wastewater treatment (19). These characteristics make ferrate(VI) a popular agent for wastewater treatment. Adsorption processes is another popular method to remove dye from wastewater (21). Among different type of adsorbents, nanoadsorbents can produce a large surface area which helps to adsorb a higher amount of pollutants from wastewater. Nanoadsorbents are effective compounds for the removal of heavy metal ions/dyes from wastewater/ aqueous solutions (22). For instance, MgO nanoparticles are effective absorbents for the removal of methyl orange from wastewater (23). Although nanoadsorbents such as MgO nanoparticles are known as an appropriate adsorbent for pollutants removal, their side effects are not fully understood. Additionally, the removal of nanoparticles from treated wastewater is not easy. Ultraviolet radiation (UV) radiation is another method for dye removal from wastewater. The UV is a powerful light which is able to

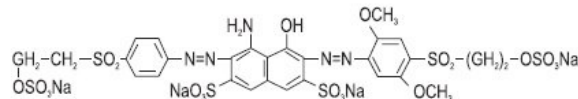


**Figure 1.** Molecular Structure of Reactive Blue 203.

break organic molecules. UV radiation is commonly used in combination with photocatalytic oxidants such as TiO<sub>2</sub>. Unfortunately, there is not enough knowledge about using UV radiation alone for wastewater treatment. The UV radiation is able to kill microorganisms; therefore, it is used for water disinfection. However, it is not a cheap and simple method for wastewater treatment (24). Sometimes, the equipment for the treatment of wastewater using UV radiation cannot be easily found in developing countries.

To date, no study has examined the removal of Reactive Blue 203 dye from wastewater by ferrate(VI) oxidation process, UV radiation, and adsorption on MgO nanoparticles. Therefore, this study investigated the effect of pH, temperature and contact time on the removal of dye from synthetic wastewater using ferrate(VI) oxidation process, UV radiation, and adsorption on MgO nanoparticles.

## 2. Materials and Methods

### 2. 1. Analytical Methods

The UV radiation was measured using digital UV meter model GBT5/OF RG3 8W made in Italy. The concentration of Reactive Blue 203 dye was measured by a spectrophotometer model UV-2100 made in Japan at a wavelength of 631 nm (25). To measure the amount of UV radiation, a GBT5/OFRG3 8W UV meter was used. A lamp emitting monochromatic UV light at a fixed wavelength (254 nm) was used for UV radiation in the experiments. The reagents and chemicals except Reactive Blue 203 were purchased from Merck. Reactive Blue 203 was purchased from the Alwan Company (Hamedan, Iran). Equation (1) was used to calculate dye removal efficiency for all of the experiments in this study.

$$RE = \frac{C_1 - C_2}{C_1} \times 100 \quad (1)$$

Where RE is the dye removal efficiency (%), C<sub>1</sub> is initial dye concentration (mg/L) and C<sub>2</sub> is the final dye concentration (mg/L). The Brunauer-Emmett-Teller (BET) surface area was determined by the adsorption of nitrogen at -196°C using a BELCAT-A apparatus operating in the single-point mode. Prior to the analysis, the samples were degassed for 2 hours at 200°C. The morphologies of calcined catalysts were determined by SEM, using an electron microscope (Vega II XMU, TESCAN) operating in backscattered and secondary electron detection modes. XRD experiments were performed with a Philips PW-1800 diffractometer using Cu Kα radiation ( $\lambda = 0.1542$  nm) at 40 kV and 30 mA to identify the crystalline phases and calculate the

lattice parameters. Scattering intensities were measured over the angular range of 5° to 90° ( $\theta$ ) for all samples, with a step size of 0.02° ( $\theta$ ) and a counting time of 2 s/step. The diffraction spectra were indexed based on the Joint Committee on Powder Diffraction Standards (JCPDS) files.

## 2.2. UV Radiation

The experiments were designed based on the “one factor at a time” method. In the first experiment, five Erlenmeyer flasks (250 mL), each containing 100 mL distilled water, were prepared. Next, a suitable amount of Reactive Blue 203 dye was added to each flask to reach the dye concentration of 26.9 mg/L. Then, a suitable amount of hydrochloric acid or sodium hydroxide was added and the pH of the five flasks was adjusted to 1, 4, 7, 11 and 13, respectively. The flasks were exposed to UV radiation using a UV lamp with an intensity of 130 mW/m<sup>2</sup> at 25°C for 15 minutes. Finally, the concentration of dye was measured using spectrophotometry.

The experiments that follow are based on the “one factor at a time” method and evaluate the effect of the temperature on the Reactive Blue 203 dye removal by UV radiation.

In the second experiment, the pH was adjusted to 13 in all flasks by adding a suitable amount of sodium hydroxide. Then, all flasks were exposed to UV radiation using a UV lamp with an intensity of 130 mW/m<sup>2</sup> for 15 minutes at temperatures of 25, 30, 40, 45 and 50°C, respectively.

The third experiment investigated the effect of contact time ranging from 1 to 65 minutes on Reactive Blue 203 dye removal by UV radiation. In this section of the study, the experiments were carried out using a UV lamp with a radiation intensity of 130 mW/m<sup>2</sup> at a temperature of 25°C. The pH of 13 and the initial dye concentration of 26.9 mg/L were used. In these experiments, the intensity of UV radiation varied from 15 to 130 mW/m<sup>2</sup>. This experiment was performed at a temperature of 25°C, a contact time of 15 minutes and a pH of 13.

## 2.3. Ferrate(VI)

The fourth experiment focused on optimizing pH, ferrate(VI) concentration, contact time and temperature for Blue 203 dye removal by ferrate(VI) oxidation process. The initial dye concentration for all the experiments was 26.9 mg/L. A series of experiments was designed to find the effect of pH on the removal of Reactive Blue 203 dye from wastewater using ferrate(VI) oxidation process under the following condition: pH was varied from 1 to 13, the temperature was 25°C and a contact time was 15 minutes. Ferrate(VI) concentrations of 0.014, 0.029, 0.044, 0.059, 0.074, 0.104, 0.118 and 0.133 mg/L were employed to find the best concentration. The conditions for these experiments were the temperature of 25°C, contact time of 15 minutes and pH of 2. Another set of

experiments was designed to evaluate the effect of contact time in the range of 1 to 25 minutes on Reactive Blue 203 dye removal from wastewater by ferrate(VI) oxidation process. In the experiments conducted to investigate the best contact time, the pH and temperature were 2 and 25°C, respectively. Eventually, temperatures of 20, 30, 40, 50, 60 and 70°C were considered to investigate the best temperature for ferrate(VI) oxidation process with a pH of 2 and contact time of 15 minutes.

## 2.4. MgO Nanoparticles

### 2.4.1. MgO Nanoparticles Generation

Nanoparticles are typically produced by sol-gel and hydrothermal methods. In this study, the sol-gel method was used to produce MgO nanoparticles by adding 100 g of MgCl<sub>2</sub>.6H<sub>2</sub>O and 50 mL of 1 N sodium hydroxide to 500 mL distilled water. The solution was mixed using magnetic stirrer at 200 rpm for 4 hours. As the sedimentation and precipitation occurred, the sediments were separated from the solution by centrifuging at 3000 rpm for 5 minutes. The separated sediments were washed with distilled water several times and dried at 60°C for 24 hours. To obtain MgO nanoparticles, the dried powder was calcined at 450°C for 2 hours. Scanning electron microscope (SEM) was used to determine the production of nanoparticles and their dimension. The specific surface area of MgO nanoparticles was measured using the BET equation applied to the adsorption data (26). Moreover, to investigate the pattern of MgO particles, X-ray diffraction (XRD) was used.

### 2.4.2. Experimental Procedures for MgO Nanoparticles

In the fifth experiment, the initial dye concentration for all the attempts was 26.9 mg/L, and the goal was to optimize pH, concentration of MgO nanoparticles, contact time and temperature for Reactive Blue 203 dye removal by adsorption process. The pH values of 1.5, 2.5, 4.5, 9, 10 and 13 were selected to find the best pH to remove Reactive Blue 203 dye from wastewater by MgO nanoparticles. The contact time, MgO nanoparticles concentration and temperature were 15 min, 133.3 mg/L and 25°C, respectively. The MgO nanoparticles concentrations of 2.45, 4.95, 7.43, 9.91, 12.39, 14.87 and 17.35 mg/L were used to investigate the best adsorbent concentration at the pH of 13, temperature of 25°C and contact time of 15 minutes. A contact time between 1 and 50 minutes was considered to be the best contact time at a pH of 13 and the temperature of 25°C.

Adsorption processes can be described by equations that are called isotherms. In this study, Langmuir, Freundlich, Temkin, Generalized, and D-R isotherms were used. The Freundlich isotherm is an empirical equation shown in equation (2).

$$\log\left(\frac{x}{m}\right) = \log K_f + \frac{1}{n} \log(C_e) \quad (2)$$

Where  $x/m$  is the amount of absorbed dye per weight of the adsorbent,  $C_e$  is the equilibrium concentration of the adsorbed dye in the solution after adsorption and  $n$  and  $K_f$  are the constant coefficients of the Freundlich isotherm. Equation 2 is analogous to the equation  $Y = a(X)+b$ , where  $a$  is defined as the slope,  $b$  is the intercept of the curve  $\log(x/m)$  versus  $\log(C_e)$ ,  $Y$  is  $\log(x/m)$ , and  $X$  is  $\log(C_e)$ . Langmuir isotherm is shown in equation 3.

$$\frac{C_e}{(x/m)} = \frac{1}{ab} + \frac{1}{a} C_e \quad (3)$$

In equation 4, the parameters  $a$  and  $b$  are Langmuir constants. Equation 4 is similar to the equation  $y=ax+b$ . By plotting  $C_e/((x/m))$  versus  $C_e$ , the  $a$  and  $b$  constants can be calculated. The Temkin isotherm is shown in equation 4. The constants  $K_T$  and  $B_1$  can be calculated using a linear plot of  $q_e$  versus  $\ln(C_e)$ .

$$qe = B_1 \ln(K_T) + B_1 \ln(C_e) \quad (4)$$

Where  $K_T$  is the equilibrium binding constant ( $L/mg$ ) corresponding to the maximum binding energy and its value rises with the increase in temperature. Constant  $B_1$  is related to the heat of adsorption. "The D-R isotherm, apart from being analogue of Langmuir isotherm, is more general than Langmuir isotherm as it rejects the homogenous surface or constant adsorption potential" (27). The D-R isotherm is shown in equation 5.

$$\ln q_e = \ln q_s - B\varepsilon^2 \quad (5)$$

Where  $q_e$  is D-R constant and  $\varepsilon$  can be calculated using equation 6.

$$\varepsilon = RT \ln \left( 1 + \frac{1}{C_e} \right) \quad (6)$$

Where  $q_e$  is the maximum amount of adsorbate that can be adsorbed by the adsorbent,  $B$  is the constant related to energy,  $C_e$  is the equilibrium concentration ( $mg/L$ ),  $R$  is the universal gas constant that is equal to  $8.314 \text{ J/mol.K}$  and  $T$  is the temperature in Kelvin. The Generalized isotherm is shown in equation 7.

$$\ln \left[ \left( \frac{q_{max}}{q_e} \right) - 1 \right] = \ln(K_G) - N \ln(C_e) \quad (7)$$

Where  $K_G$  is the saturation constant ( $mg/L$ ),  $N$  is the cooperative binding constant,  $q_{max}$  is the maximum adsorption capacity of the adsorbent ( $mg/g$ ) and  $q_e$  ( $mg/g$ ) and  $C_e$  ( $mg/L$ ) are the equilibrium dye concentrations in the soil and liquid phases, respectively. The values of  $N$  and  $K_G$  are calculated from the slopes and intercepts of the plots.

### 3. Results and Discussion

#### 3. 1. UV Radiation

##### 3. 1. 1. The Effect of pH

pH has been reported as one of the effective parameters

for the removal of pollutants from wastewater using UV radiation (28). The results of this study showed that increasing pH resulted in improved dye removal efficiency by UV radiation. As shown in Figure 2a, the increase of pH from 1 to 7 had no significant effect (only 10% to 20%) on the efficiency of dye removal using UV radiation. Meanwhile, increasing pH from 7 to 11 boosted dye removal efficiency up to 36%. Hence, as pH reached 13, the dye removal efficiency increased to 80%. Similarly, Talaiekhozani et al reported that increasing pH leads to an increase in the removal of hydrogen sulfide and COD in domestic wastewater by UV radiation (28). As reported by Nekouei and Nekouei, the highest removal of dye (methylene blue) was 98.88% at pH 6 under UV light (29). It has been reported that the dye removal from wastewater is higher at a pH greater than 7 using UV radiation (30, 31). It has also been found that in highly alkaline conditions ( $pH > 10$ ), the probability of  $^{*}\text{OH}$  radical formation increases. This radical acts as a strong oxidant and improves the process of UV degradation (32-35). It was reported that in acidic conditions, UV cannot be effective due to the absorption of UV radiation by the high concentration of hydronium ( $\text{H}_3\text{O}^+$ ) cations (36). In alkaline conditions, the concentration of hydroxyl ion ( $\text{OH}^-$ ) increase and the concentration of  $\text{H}_3\text{O}^+$  decrease (37). For this reason, UV radiation is more effective in alkaline condition.

##### 3. 1. 2. The Effect of Temperature

The previous studies showed that the temperature increases the removal of dye from wastewater (38-41). In contrast, several studies reported a negative effect of increasing temperature on dye removal from wastewater (42-44). The effect of temperature on the removal of dye using UV radiation is shown in Figure 2b. Based on the results, changes in temperature in the range of 25 to  $50^\circ\text{C}$  had no significant effect on the increase or decrease of the removal efficiency using UV radiation. It should be noted that changes in temperature during wastewater treatment is very expensive. Therefore, only a few processes need to increase or decrease wastewater temperature. UV radiation causes the generation of reactive radicals that can oxidize organic compounds. Ghodbane and Hamdaoui believe that UV radiation is able to remove the dye due to the generation of the free radical or free electron on the molecules of dye (36). Additionally, they reported that a negative charge has appeared on the dye molecules under UV radiation. Increasing or decreasing temperature does not have a significant effect on the generation of such radicals. Therefore, the temperature was not considered as an effective factor in dye removal using UV radiation.

##### 3. 1. 3. The Effect of Contact Time

Contact time is an important parameter in designing the appropriate volume of the reactor in wastewater treatment systems when UV radiation is used (45). As

shown in Figure 2c, increasing the contact time from 1 to 15 minutes had a significant effect on the dye removal efficiency from wastewater. However, by increasing contact time to between 15 and 65 minutes, not much effect on Reactive Blue 203 dye removal efficiency was observed. The removal efficiency in 1 minute was only 5%, while it reached 86% at 15 minutes. In addition, increasing contact time up to 65 minutes resulted in 95% removal efficiency, which was only 10% higher than the contact time of 15 minutes. Therefore, these results showed that the best contact time was 15 minutes for the removal of Reactive Blue 203 dye using UV radiation. Similar results were reported by Talaiekhozani et al (37). They investigated the removal of Reactive Blue 203 dye from wastewater using UV radiation and reported that the best contact time for dye removal using UV radiation was around 15 minutes.

### 3. 1. 4. The Effect of UV Radiation Intensity

The intensity of UV radiation is one of the effective parameters in the removal of dye from wastewater. Figure

2d shows the effect of UV radiation intensity on the removal of Reactive Blue 203 dye. In UV radiation of 15 mW/m<sup>2</sup>, 78% of the Reactive Blue 203 dye was removed. By increasing the UV radiation to 28 W/m<sup>2</sup>, the efficiency of dye removal increased to 88%. Hence, increasing the intensity of UV radiation to 130 mW/m<sup>2</sup> achieved 94% efficiency for dye removal using UV radiation. There are few numbers of studies on the effect of UV radiation intensity on dye removal. Behnajady et al (46) reported that there is a direct relationship between UV radiation and azo dye removal. They reported that a higher intensity of UV radiation means higher azo dye removal.

## 3. 2. Ferrate(VI)

### 3. 2. 1. The Effect of pH

The results of this study showed that pH is one of the most important parameters for the removal of Reactive Blue 203 dye from wastewater using ferrate(VI) oxidation process. As shown in Figure 3a, at pH 1, the removal rate was 38%, while by increasing pH to 13, the removal efficiency was only 7%. The dye removal efficiency at

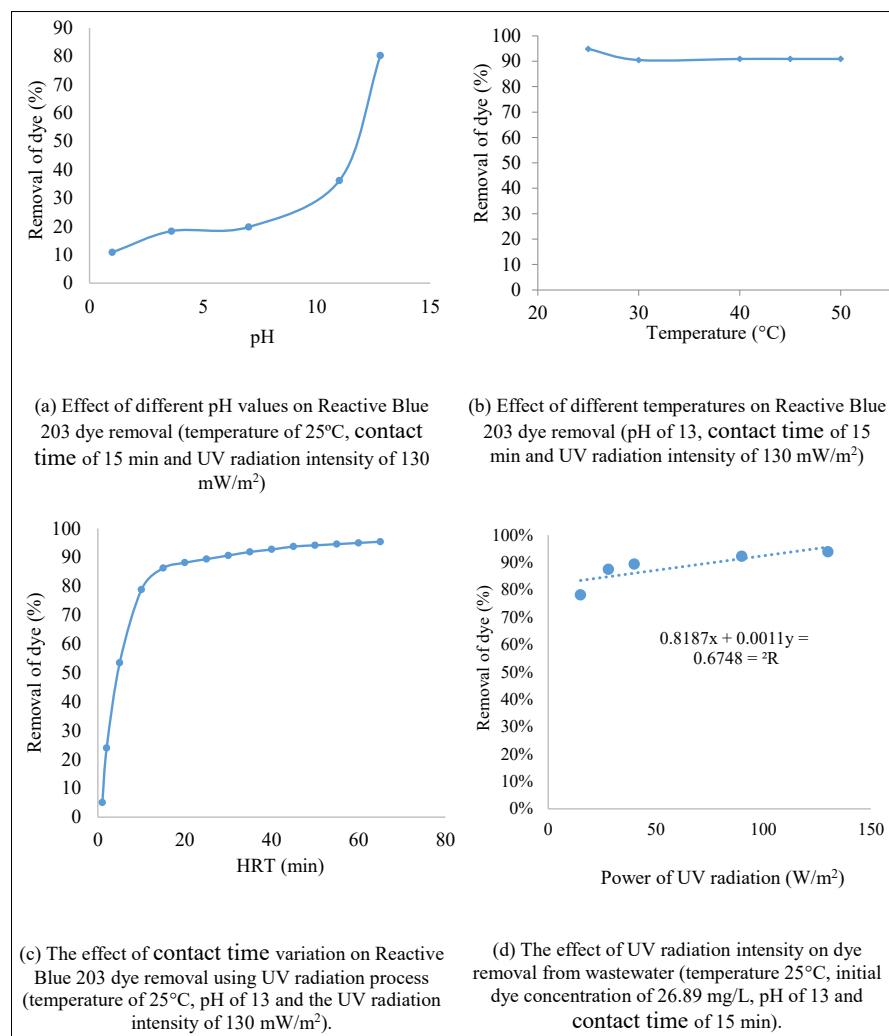
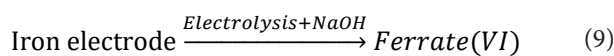


**Figure 2.** Effect of Temperature, Contact Time and pH on Reactive Blue 203 Dye Removal Using UV Radiation and Oxidation Process

different pH values can be calculated using equation 8 when the ferrate(VI) oxidation process is used. It should be noted that this equation is a linear form which is applied in a special range, therefore, it could not be employed in all conditions.

$$y = -2.2945x + 39.092 \quad (R^2 = 0.96) \quad (8)$$

Where  $y$  is Reactive Blue 203 dye removal efficiency (%) and  $x$  is the pH of the wastewater. Talaiekhozani et al reported similar results about the effects of pH on the removal of formaldehyde, COD and hydrogen sulfide from wastewater using ferrate(VI) oxidation process (47). Although ferrate(VI) in acidic conditions is highly capable of removing Reactive Blue 203 dye from wastewater, the cost of pH reduction is very high. They also calculated the cost of pH reduction in domestic wastewater using sodium hydroxide (19). The fact that in an acidic pH, ferrate(VI) is more capable of removing dye from wastewater can be explained as follows. According to equation 9, ferrate(VI) is produced by electrolysis of distilled water using iron electrodes in the presence of sodium hydroxide.



Ferrate(VI) production leads to the formation of a purple color in the sodium hydroxide and water solution. Ferrate(VI) can be produced in two forms, specifically the inorganic anion  $\text{FeO}_4^{2-}$  and the protonated ferrate  $\text{HFeO}_4^-$ . The rate constant of each of the two ferrate(VI) species can be calculated by equation 11. In equation 10,  $K_1$  and  $K_2$  are the rate constants of  $\text{HFeO}_4^-$  and  $\text{FeO}_4^{2-}$ .

$$K[\text{Ferrate}] = K_1[\text{HFeO}_4^-] + K_2[\text{FeO}_4^{2-}] \quad (10)$$

The rate constants of  $\text{HFeO}_4^-$  and  $\text{FeO}_4^{2-}$  are  $1.24 \times 10^7 \text{ m/s}$  and  $8.41 \times 10^2 \text{ m/s}$ , respectively. As a result, the reaction rate between Reactive Blue 203 dye and  $\text{HFeO}_4^-$  is higher compared with  $\text{FeO}_4^{2-}$  (19). Therefore,  $\text{HFeO}_4^-$  has a higher contribution in removing dye from wastewater. In acidic conditions,  $\text{HFeO}_4^-$  is the dominant form of ferrate(VI) in wastewater, while in alkaline conditions  $\text{FeO}_4^{2-}$  is the more dominant form. In acidic environment, ferrate(VI) could be more effective in removing Reactive Blue 203 dye from wastewater because of the presence of  $\text{HFeO}_4^-$  (19).

### 3.2.2. The Effect of Contact Time

Contact time is one of the important parameters essential to determine the volume of wastewater treatment reactors on a large scale (19). The effect of contact time on dye removal using ferrate(VI) oxidation process is shown in Figure 3b. The reaction time can be categorized as a rapid reaction. In these conditions, the only effective parameter for removing Reactive Blue 203 dye from wastewater is mass transfer. Ferrate(VI) after entering the

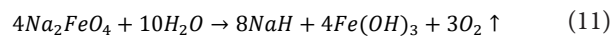
reactor required a time to be dispersed by the agitators in wastewater. This duration depends only on the efficiency of the mixer and its power. According to Talaiekhozani et al, the contact time of 60 minutes is the best for the removal of hydrogen sulfide and COD from domestic wastewater using ferrate(VI) (48). These results indicate that the effect of contact time on the removal of pollutants by ferrate(VI) depends on the type of pollutant.

### 3.2.3. The Effect of Temperature

In this study, the effect of temperature on dye removal using ferrate(VI) was investigated. The results showed that by increasing temperature up to 50°C, the dye removal efficiency using ferrate(VI) was increased (Figure 3c). The dye removal efficiency at 20°C was only 45% and at 50°C it was 85%. Eskandari (2016) investigated the conversion rate of ferrate(VI) to ferric(III) at different temperatures (19). They found that the conversion rate of ferrate(VI) at temperatures between 20 and 50°C did not change much, but may increase significantly at temperatures over 50°C. Although ferric(III) is a powerful coagulant, it does not have the ability to oxidize organic or inorganic compounds (28). For this reason, when the temperature increased to more than 50°C, the removal efficiency for Reactive Blue 203 dye decreased dramatically. Similar results showed that the efficiency of pollutants removal at temperatures less than 50°C increased and the pollutants removal at temperatures above 50°C decreased when ferrate(VI) oxidation process is used (47).

### 3.2.4. The Ratio of Ferrate(VI) to Dye

In this study, ferrate(VI) was produced by an electrochemical process. Since the electrolytic medium contained only sodium hydroxide and iron electrodes, the produced ferrate(VI) was sodium ferrate ( $\text{Na}_2\text{FeO}_4$ ). According to equation 11, sodium ferrate is slowly converted to iron(III) oxide-hydroxide ( $\text{Fe(OH)}_3$ ) and oxygen ( $\text{O}_2$ ). Iron(III) oxide-hydroxide is a powerful coagulant compound that can remove suspended particles from wastewater (49). Therefore, the use of ferrate(VI) leads not only to the oxidation of organic compounds and some inorganic compounds in wastewater but also to the removal of suspended particles. During wastewater treatment using ferrate(VI), oxygen is released, which can increase dissolved oxygen (DO) concentration in wastewater. A higher concentration of DO in wastewater can prevent the formation of anaerobic conditions and odor in other parts of the wastewater treatment plant (50).



The inadequacy of ferrate(VI) during wastewater treatment leads to a reduction in dye removal efficiency, while excessive ferrate(VI) leads to higher costs. Therefore, it is important to determine the optimal ratio of ferrate(VI) to dye. As shown in Figure 3d, when the

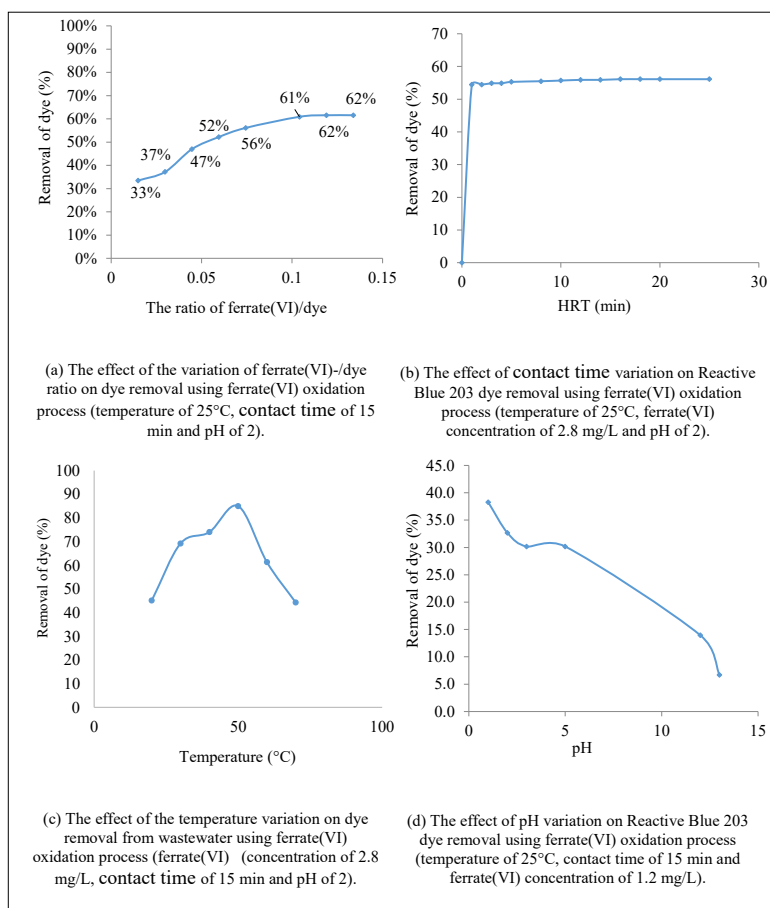


**Figure 3.** The Effects of pH, Ratio of Ferrate(VI) to Dye, Contact Time and Temperature and Intensity of UV Radiation on the Removal of Dye Using Ferrate(VI) Oxidation Process

ratio of ferrate(VI) to dye is equal to 0.01, the dye removal efficiency was 33%. By increasing the ratio of ferrate(VI) to dye to 0.1, dye removal efficiency reached 61%. The results showed that the efficiency did not increase with an increase in the ratio of ferrate(VI) to dye to more than 0.1. Talaiekhozani et al showed that increasing ferrate(VI) concentration to 1.68 mg/L leads to the removal of 100 and 62% of hydrogen sulfide and COD from domestic wastewater, respectively (28).

### 3. 3. MgO Nanoparticles

#### 3. 3. 1. SEM Analysis of MgO Nanoparticles

The surface morphology and texture of MgO nanoparticles by SEM image is shown in Figure 4a. SEM analysis showed that the size of MgO nanoparticles was in the range of 42 to 64 nm, which are categorized as nanomaterial size.

Based on Scherrer equation, the average crystalline size of the particles was found to be roughly 60 nm. All peaks in the XRD pattern of MgO were very sharp with no impurity peaks and the crystalline phase was completely formed. Peak intensities in Figure 4b revealed that the total scattering from each plane in the phase's crystal structure was related to the distribution of

particular atoms in the structure. The diffraction peaks corresponding to crystalline MgO appeared at  $2\theta = 37.11$ , 43.0, 50.21 and 73.79°. This pattern showed that a single cubic phase was consistent with the standard spectrum of cubic MgO (JCPDS card no: 45-0946) (51). The specific surface area of MgO nanoparticles was measured using the BET equation applied to the adsorption data (52). The results showed that the average specific surface area of MgO nanoparticles was 102.6 m<sup>2</sup>/g.

#### 3. 3. 2. The Effect of pH, Temperature, Contact Time and Ratio of MgO Nanoparticles to Dye

Figure 5a shows that increasing the pH of the environment leads to an increase in the adsorption of Reactive Blue 203 dye on MgO nanoparticles at pH 13. Mousavi and Mahmoudi reported that MgO nanoparticles have the ability to absorb the Reactive Blue 19 and Red 198 dyes (53). In addition, they stated that MgO nanoparticles can remove 98% of these dyes from wastewater at pH 8. The results showed that only 15% of Reactive Blue 203 dye was absorbed at pH 8 from the MgO nanoparticles. As mentioned above, increasing the pH of wastewater is costly and can lead to a sharp increase in wastewater treatment costs (19).

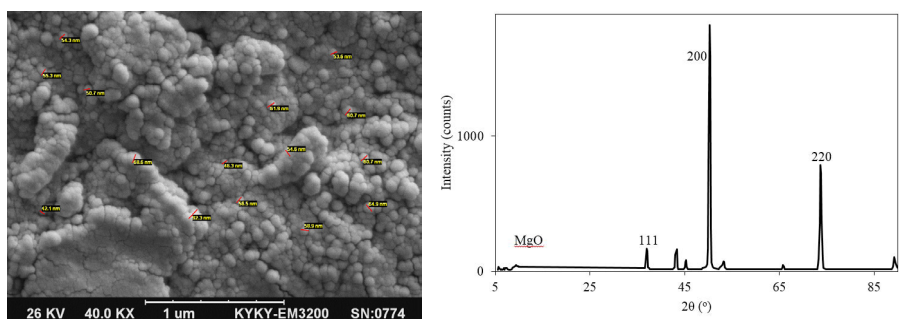


**Figure 4.** (a) SEM Image of Synthesized MgO Nanoparticles and (b) XRD of Synthesized MgO Nanoparticles

Nanoparticles have a large surface area due to their small size, so they can be considered as adsorbent (54). The results showed that increasing the ratio of nanoparticles to the concentration of dye from 2.24 to 12.39 resulted in an increase in dye removal from wastewater (Figure 5b). However, increasing the ratio of nanoparticles to the concentration of dye to higher than 12.39 had no effect on dye removal efficiency. The ratio of nanoparticles to the concentration of dye equal to 12 was the best value. The results showed that using a higher ratio of nanoparticles

to dye had no significant effect on dye adsorption on MgO nanoparticles. In this study, the best concentration of MgO nanoparticles was about 333 mg/L. The maximum adsorption capacities of MgO nanoparticles were 166.7 and 123.5 mg of dye per gram of adsorbent for Reactive Blue 19 and Reactive Red 198, respectively (53).

Temperature has been introduced as an effective parameter in absorbing pollutants on different adsorbents. Normally, lower temperatures result in higher adsorption of pollutants in physical adsorption (55). The results of

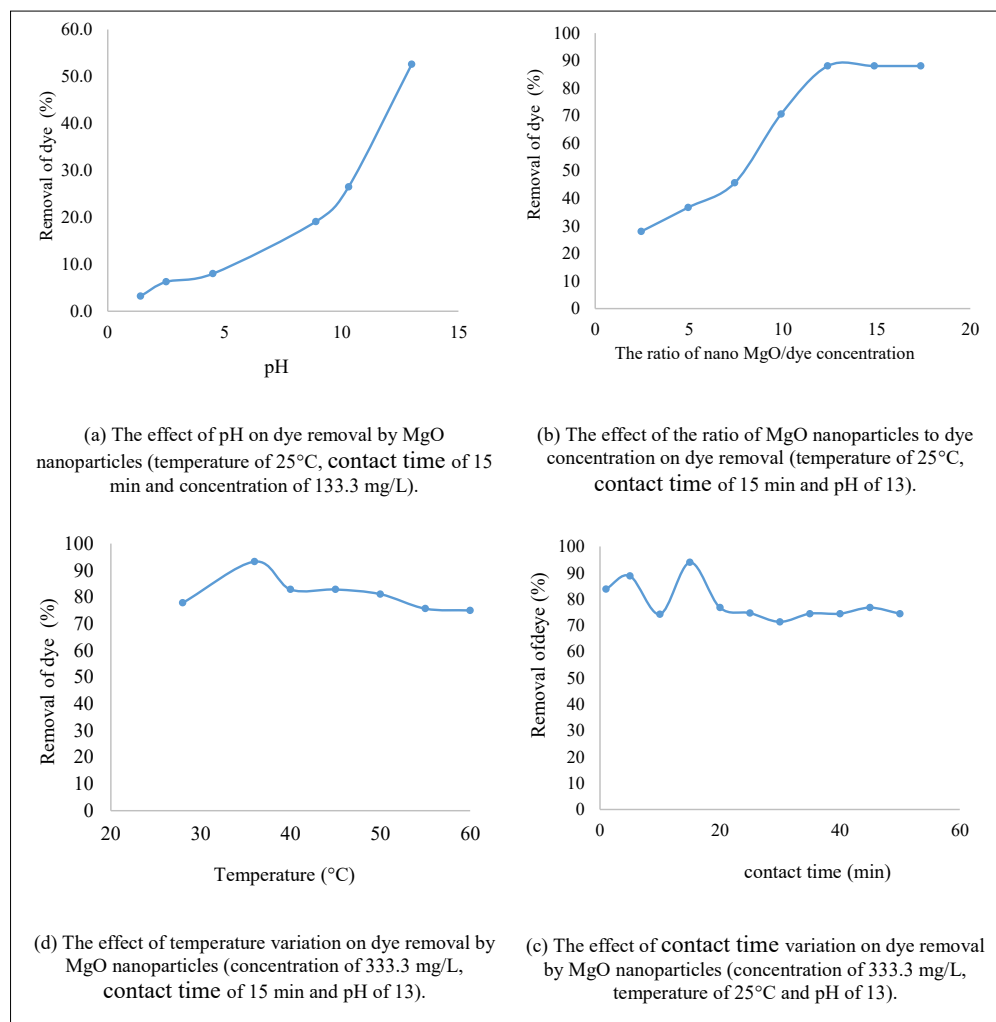


**Figure 5.** The Effect of pH, Temperature, Contact Time and MgO Nanoparticles Concentration on Reactive Blue 203 Dye Removal

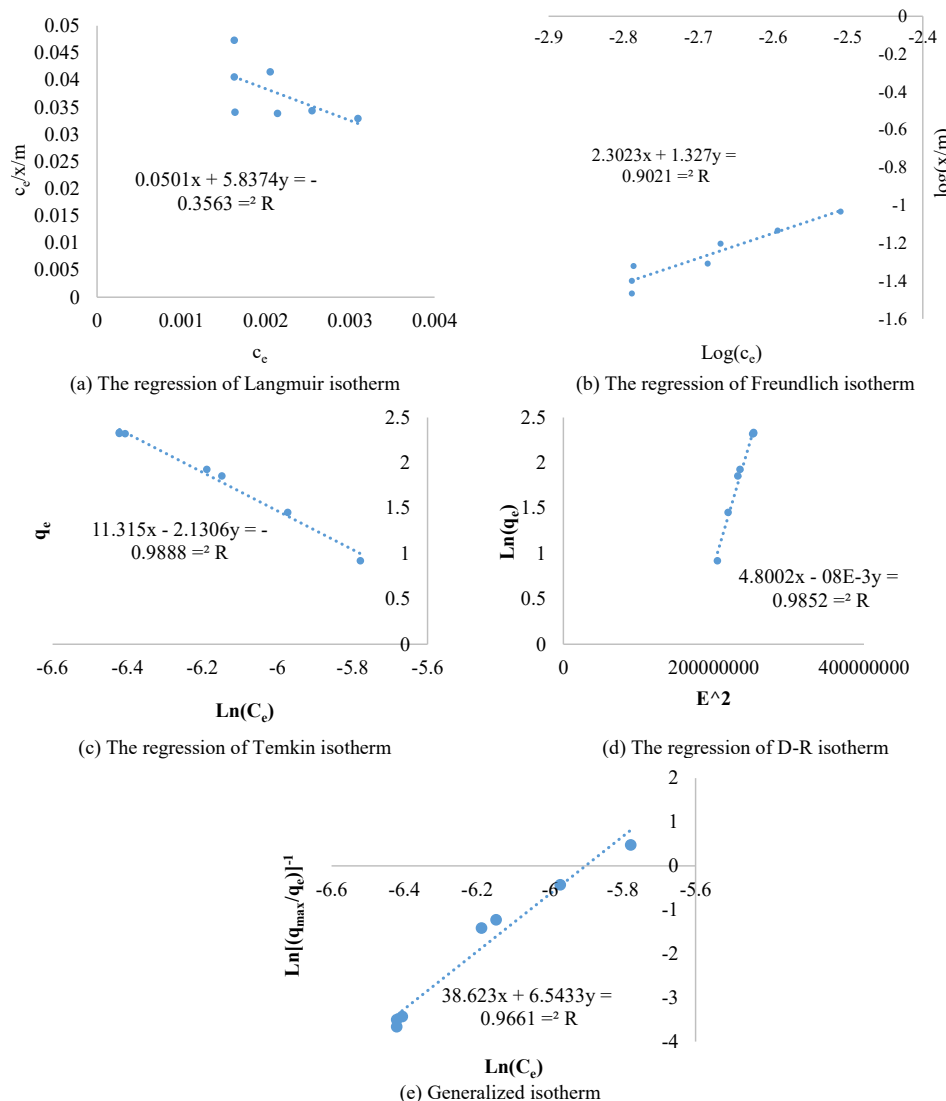
this study showed that changes in temperature from 28 to 60°C had a slight effect on the dye adsorption on the MgO nanoparticles (Figure 5c). An increase in temperature between 28 and 60°C showed a reduction in adsorption efficiency from 78% to 60%, respectively.

Figure 5d shows the effect of different contact time ranging from 1 to 50 minutes on Reactive Blue 203 dye removal from wastewater. Contact time had no significant effect on the adsorption of Reactive Blue 203 dye from wastewater by MgO nanoparticles. The results indicated that Reactive Blue 203 dye adsorption onto MgO nanoparticles was completed in less than 1 minute. Mousavi and Mahmoudi reported that MgO nanoparticles can remove 98% of both Reactive Blue 19 and Reactive Red 198 at a contact time of 5 minutes (53). Hu et al found that for the removal of Congo Red dye with an initial concentration of 100 mg/L using nanoparticles of MgO, a contact time of 30 minutes is required (56).

### 3.3.3. Adsorption Isotherms

Langmuir, Freundlich, Temkin, Generalized and D-R isotherms were examined for the removal of Reactive Blue 203 dye from wastewater by MgO nanoparticles (Figure 6). The best isotherm to describe the dye removal by MgO nanoparticle was selected based on correlation coefficients ( $R^2$ ). The constant coefficients of Langmuir, Freundlich, Generalized, and Temkin isotherms in this study are shown in Table 1.

Table 1 shows that the correlation coefficient in the Temkin isotherm was higher compared to the Freundlich, Langmuir, Generalized, and D-R isotherms. These results indicate that dye removal using MgO nanoparticles could be described by the Temkin isotherm. The Temkin isotherm proposes a linear reduction of adsorption/desorption energy as the degree of adsorption/desorption on the surface of adsorbent increases. This model in comparison to other isotherm tries to focus on the presence of indirect interaction between of adsorption



**Figure 6.** The Results of Langmuir, Freundlich, Temkin and D-R Isotherms for Reactive Blue 203 Dye Adsorption Using MgO Nanoparticles

**Table 1.** Constant Coefficients of Isotherms for Removal of Reactive Blue 203 Dye by MgO Nanoparticles

Langmuir			Freundlich			Temkin			D-R			Generalized		
a	b	R <sup>2</sup>	k <sub>f</sub>	n	R <sup>2</sup>	K <sub>T</sub>	B <sub>1</sub>	R <sup>2</sup>	q <sub>e</sub>	B	R <sup>2</sup>	N	K <sub>G</sub>	R <sup>2</sup>
0.171	0.0001166	0.35	200	0.0753	0.90	2024.4	-2.1306	0.99	0.00822	3×10 <sup>-0.08</sup>	0.98	6.5433	5.9395×10 <sup>16</sup>	0.96

and adsorbent and states that due to these interactions, the enthalpy of adsorption of all molecules in the layer would be reduced linearly with coverage (57). It should be noted that adsorption of dye on the surface of MgO proved the presence of indirect adsorbate/adsorption. K<sub>T</sub> is the equilibrium binding constant (L/mg) related to maximum binding energy and the value increases with an increase in the temperature. Constant B<sub>1</sub> describes the enthalpy of adsorption (57). The value of each parameter is defined in Table 1. Therefore, the heat of adsorption of all dye in the layer would decrease linearly with coverage. In contrast, Mousavi and Mahmoudi reported that the removal of Reactive Blue 19 and Reactive Red 198 dye by MgO nanoparticles was described by the Langmuir isotherm. In their study, they showed that the maximum adsorption capacity of MgO nanoparticles predicted for the removal of the Reactive Blue 19 was 166.7 mg/g and it was 123.5 mg/g for Reactive Red 198 dye. Hu et al showed that the removal of the Congo Red dye by MgO nanoparticles can be described by the Langmuir isotherm with a maximum adsorption capacity of 131 mg/g.

### 3. 4. Comparison of the Methods

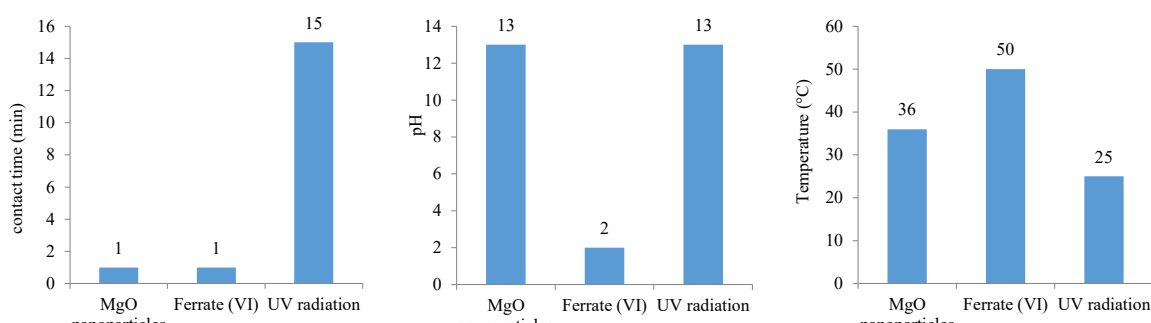
The best contact time for the three methods of adsorption, namely MgO nanoparticles, ferrate(VI) oxidation process, and UV radiation, is shown in Figure 7a. The best contact time was 1 minute for the removal of Reactive Blue 203 dye by adsorption using MgO nanoparticles and ferrate(VI) oxidation process, while it was 15 minutes using UV radiation. The shortest contact time, about 1 minute, was related to the adsorption processes on the MgO nanoparticles and ferrate(VI) oxidation process.

Figure 7b shows that pH 13 was the best for adsorption on MgO nanoparticles and UV radiation. Meanwhile, pH 2 was optimal for the removal of the Reactive Blue 203 dye by ferrate(VI) oxidation process. Talaiekhozani et al reported that the cost of reducing pH 2 for each cubic meter of domestic wastewater is approximately US\$2.52 (58). The removal efficiencies of Reactive Blue 203 from wastewater by adsorption on MgO nanoparticles, the ferrate(VI) oxidation process and UV radiation at pH 7 were 15%, 26% and 20%, respectively.

The best temperatures for the removal of Reactive Blue 203 dye from the wastewater by adsorption on the MgO nanoparticles and UV radiation were 36°C and 25°C, respectively. The best temperature for ferrate(VI) oxidation process was 50°C (Figure 7c). The results showed that UV radiation had the best temperature near the ambient temperature. If the average ambient temperature is assumed to be 20°C, the removal efficiencies of Reactive Blue 203 dye by adsorption on MgO nanoparticles, ferrate(VI) oxidation process and UV radiation at ambient temperature were 85%, 45% and 94%, respectively. Therefore, UV radiation at ambient temperature showed the highest dye removal efficiency.

### 4. Conclusion

This study focused on Reactive Blue 203 dye removal from synthetic wastewater using UV radiation, ferrate(VI) oxidation process, and adsorption on MgO nanoparticles. The alkaline environment was the best condition for the removal of Reactive Blue 203 dye from wastewater using UV radiation and adsorption on MgO nanoparticles while the acidic environment can enhance the ferrate(VI) oxidation process. Although the temperature was



(a) The comparison of contact time in three methods for Reactive Blue 203 dye removal

(b) The comparison of pH in three methods for Reactive Blue 203 dye removal

(c) The comparison of temperature in three methods for Reactive Blue 203 dye removal

**Figure 7.** The Comparison of the Best Contact Time, pH and Temperature in Three Methods of Adsorption on MgO Nanoparticles, Ferrate(VI) Oxidation Process and UV Radiation

not an effective parameter for dye removal using UV radiation and adsorption on MgO nanoparticles, it is an effective factor for ferrate(VI) oxidation process. The best temperature for Reactive Blue 203 dye removal by ferrate(VI) oxidation process was 50°C. This study showed that UV radiation needs several minutes to be completed while Reactive Blue 203 dye removal using ferrate(VI) oxidation process and MgO nanoparticles did not depend on contact time. It means that contact time was not an effective factor in the removal of dye using ferrate(VI) oxidation process and adsorption on MgO nanoparticles. Oxidation of Reactive Blue 203 dye could be categorized as a quick reaction. The maximum removals of Reactive Blue 203 dye using UV radiation, ferrate(VI) oxidation process and MgO nanoparticles were 95%, 85% and 94%, respectively. It was also found that Reactive Blue 203 dye adsorption by MgO nanoparticles can be described by Temkin isotherm. It should be noted that dye concentration is an important factor in dye removal that should be investigated. Therefore, we recommended that this factor should be evaluated in future studies.

#### Conflict of Interest Disclosures

The authors declare that they have no conflict of interests.

#### Acknowledgements

This study was extracted from the thesis by Nilofar Torkan, a student of chemical engineering in the Jami Institute of Technology (JIT), Isfahan, Iran. The authors of this study appreciate the financial and spiritual support provided by JIT.

#### References

- Jorfi S, Darvishi Cheshmeh Soltani R, Ahmadi M, Khataee A, Safari M. Sono-assisted adsorption of a textile dye on milk vetch-derived charcoal supported by silica nanopowder. *J Environ Manage.* 2017;187:111-21. doi: [10.1016/j.jenvman.2016.11.042](https://doi.org/10.1016/j.jenvman.2016.11.042).
- Georgiou D, Melidis P, Aivasidis A, Gimouhopoulos K. Degradation of azo-reactive dyes by ultraviolet radiation in the presence of hydrogen peroxide. *Dyes Pigm.* 2002;52(2):69-78. doi: [10.1016/S0143-7208\(01\)00078-X](https://doi.org/10.1016/S0143-7208(01)00078-X).
- Jorfi S, Barzegar G, Ahmadi M, Darvishi Cheshmeh Soltani R, Alah Jafarzadeh Haghhighifard N, Takdastan A, et al. Enhanced coagulation-photocatalytic treatment of Acid red 73 dye and real textile wastewater using UVA/synthesized MgO nanoparticles. *J Environ Manage.* 2016;177:111-8. doi: [10.1016/j.jenvman.2016.04.005](https://doi.org/10.1016/j.jenvman.2016.04.005).
- Khamparia S, Jaspal DK. Adsorption in combination with ozonation for the treatment of textile waste water: a critical review. *Front Environ Sci Eng.* 2017;11(1):8. doi: [10.1007/s11783-017-0899-5](https://doi.org/10.1007/s11783-017-0899-5).
- Chen Y, Cheng JJ, Creamer KS. Inhibition of anaerobic digestion process: a review. *Bioresour Technol.* 2008;99(10):4044-64. doi: [10.1016/j.biortech.2007.01.057](https://doi.org/10.1016/j.biortech.2007.01.057).
- Horst MF, Lassalle V, Ferreira ML. Nanosized magnetite in low cost materials for remediation of water polluted with toxic metals, azo- and antraquinonic dyes. *Front Environ Sci Eng.* 2015;9(5):746-69. doi: [10.1007/s11783-015-0814-x](https://doi.org/10.1007/s11783-015-0814-x).
- Crini G. Non-conventional low-cost adsorbents for dye removal: a review. *Bioresour Technol.* 2006;97(9):1061-85. doi: [10.1016/j.biortech.2005.05.001](https://doi.org/10.1016/j.biortech.2005.05.001).
- Mozia S, Tomaszewska M, Morawski AW. A new photocatalytic membrane reactor (PMR) for removal of azo-dye Acid Red 18 from water. *Appl Catal B Environ.* 2005;59(1-2):131-7. doi: [10.1016/j.apcatb.2005.01.011](https://doi.org/10.1016/j.apcatb.2005.01.011).
- Gouthaman A, Azarudeen RS, Gnanaprakasam A, Sivakumar VM, Thirumurugan M. Polymeric nanocomposites for the removal of Acid red 52 dye from aqueous solutions: Synthesis, characterization, kinetic and isotherm studies. *Ecotoxicol Environ Saf.* 2018;160:42-51. doi: [10.1016/j.ecoenv.2018.05.011](https://doi.org/10.1016/j.ecoenv.2018.05.011).
- Sobana N, Swaminathan M. The effect of operational parameters on the photocatalytic degradation of acid red 18 by ZnO. *Sep Purif Technol.* 2007;56(1):101-7. doi: [10.1016/j.seppur.2007.01.032](https://doi.org/10.1016/j.seppur.2007.01.032).
- Katheresan V, Kansedo J, Lau SY. Efficiency of various recent wastewater dye removal methods: A review. *J Environ Chem Eng.* 2018;6(4):4676-97. doi: [10.1016/j.jece.2018.06.060](https://doi.org/10.1016/j.jece.2018.06.060).
- Fu R, Mu N, Guo X, Xu Z, Bi D. Removal of decabromodiphenyl ether (BDE-209) by sepiolite-supported nanoscale zerovalent iron. *Front Environ Sci Eng.* 2015;9(5):867-78. doi: [10.1007/s11783-015-0800-3](https://doi.org/10.1007/s11783-015-0800-3).
- Uyak V. Multi-pathway risk assessment of trihalomethanes exposure in Istanbul drinking water supplies. *Environ Int.* 2006;32(1):12-21. doi: [10.1016/j.envint.2005.03.005](https://doi.org/10.1016/j.envint.2005.03.005).
- Namasivayam C, Jeyakumar R, Yamuna RT. Dye removal from wastewater by adsorption on 'waste' Fe(III)/Cr(III) hydroxide. *Waste Manag.* 1994;14(7):643-8. doi: [10.1016/0956-053X\(94\)90036-1](https://doi.org/10.1016/0956-053X(94)90036-1).
- Wang S, Li H, Xu L. Application of zeolite MCM-22 for basic dye removal from wastewater. *J Colloid Interface Sci.* 2006;295(1):71-8. doi: [10.1016/j.jcis.2005.08.006](https://doi.org/10.1016/j.jcis.2005.08.006).
- Salem ANM, Ahmed MA, El-Shahat MF. Selective adsorption of amaranth dye on Fe3O4/MgO nanoparticles. *J Mol Liq.* 2016;219:780-8. doi: [10.1016/j.molliq.2016.03.084](https://doi.org/10.1016/j.molliq.2016.03.084).
- Nassar MY, Mohamed TY, Ahmed IS, Samir I. MgO nanostructure via a sol-gel combustion synthesis method using different fuels: An efficient nano-adsorbent for the removal of some anionic textile dyes. *J Mol Liq.* 2017;225:730-40. doi: [10.1016/j.molliq.2016.10.135](https://doi.org/10.1016/j.molliq.2016.10.135).
- Rai PK, Lee J, Kailasa SK, Kwon EE, Tsang YF, Ok YS, et al. A critical review of ferrate(VI)-based remediation of soil and groundwater. *Environ Res.* 2018;160:420-48. doi: [10.1016/j.envres.2017.10.016](https://doi.org/10.1016/j.envres.2017.10.016).
- Eskandari Z. Control of hydrogen sulfide and organic compounds in municipal wastewater by using ferrate (VI) produced by electrochemical method. Isfahan, Iran: Jami Institute of Technology; 2016.
- Sharma VK. Ferrate(VI) and ferrate(V) oxidation of organic compounds: Kinetics and mechanism. *Coord Chem Rev.* 2013;257(2):495-510. doi: [10.1016/j.ccr.2012.04.014](https://doi.org/10.1016/j.ccr.2012.04.014).
- Banerjee S, Chattopadhyaya MC. Adsorption characteristics for the removal of a toxic dye, tartrazine from aqueous solutions by a low cost agricultural by-product. *Arab J Chem.* 2017;10 Suppl 2:S1629-S38. doi: [10.1016/j.arabjc.2013.06.005](https://doi.org/10.1016/j.arabjc.2013.06.005).
- Nazarzadeh Zare E, Motahari A, Sillanpaa M. Nanoabsorbents based on conducting polymer nanocomposites with main focus on polyaniline and its derivatives for removal of heavy metal ions/dyes: A review. *Environ Res.* 2018;162:173-95. doi: [10.1016/j.envres.2017.12.025](https://doi.org/10.1016/j.envres.2017.12.025).
- Ge L, Wang W, Peng Z, Tan F, Wang X, Chen J, et al. Facile fabrication of Fe@ MgO magnetic nanocomposites for efficient removal of heavy metal ion and dye from water.

- Powder Technol. 2018;326:393-401. doi: [10.1016/j.powtec.2017.12.003](https://doi.org/10.1016/j.powtec.2017.12.003).
24. Tchobanoglous G, Burton FL, Stensel HD. Wastewater engineering: treatment and reuse. USA: McGraw Hill; 2003.
  25. Kalyani DC, Telke AA, Dhanve RS, Jadhav JP. Ecofriendly biodegradation and detoxification of Reactive Red 2 textile dye by newly isolated Pseudomonas sp. SUK1. *J Hazard Mater.* 2009;163(2-3):735-42. doi: [10.1016/j.jhazmat.2008.07.020](https://doi.org/10.1016/j.jhazmat.2008.07.020).
  26. Aramendia MA, Benitez JA, Borau V, Jimenez C, Marinas JM, Ruiz JR, et al. Characterization of Various Magnesium Oxides by XRD and <sup>1</sup>H MAS NMR Spectroscopy. *J Solid State Chem.* 1999;144(1):25-9. doi: [10.1006/jssc.1998.8089](https://doi.org/10.1006/jssc.1998.8089).
  27. Robati D, Mirza B, Rajabi M, Moradi O, Tyagi I, Agarwal S, et al. Removal of hazardous dyes-BR 12 and methyl orange using graphene oxide as an adsorbent from aqueous phase. *Chem Eng J.* 2016;284:687-97. doi: [10.1016/j.cej.2015.08.131](https://doi.org/10.1016/j.cej.2015.08.131).
  28. Talaiekhozani A, Eskandari Z, Bagheri M, Talaei MR, Salari M. Hydrogen sulfide and organic compounds removal in municipal wastewater using ferrate (VI) and ultraviolet radiation. *Environ Health Eng Manag J.* 2017;4(1):7-14. doi: [10.15171/EHEM.2017.02](https://doi.org/10.15171/EHEM.2017.02).
  29. Nekouei F, Nekouei S. Comparative evaluation of BiOCl-NPs-AC composite performance for methylene blue dye removal from solution in the presence/absence of UV irradiation: Kinetic and isotherm studies. *J Alloys Compd.* 2017;701:950-66. doi: [10.1016/j.jallcom.2017.01.157](https://doi.org/10.1016/j.jallcom.2017.01.157).
  30. Huang M, Xu C, Wu Z, Huang Y, Lin J, Wu J. Photocatalytic discolorization of methyl orange solution by Pt modified TiO<sub>2</sub> loaded on natural zeolite. *Dyes Pigm.* 2008;77(2):327-34. doi: [10.1016/j.dyepig.2007.01.026](https://doi.org/10.1016/j.dyepig.2007.01.026).
  31. Daneshvar N, Salari D, Khataee AR. Photocatalytic degradation of azo dye acid red 14 in water: investigation of the effect of operational parameters. *J Photochem Photobiol A Chem.* 2003;157(1):111-6. doi: [10.1016/S1010-6030\(03\)00015-7](https://doi.org/10.1016/S1010-6030(03)00015-7).
  32. Goncalves MS, Oliveira-Campos AM, Pinto EM, Plasencia PM, Queiroz MJ. Photochemical treatment of solutions of azo dyes containing TiO<sub>2</sub>. *Chemosphere.* 1999;39(5):781-6. doi: [10.1016/S0045-6535\(99\)00013-2](https://doi.org/10.1016/S0045-6535(99)00013-2).
  33. Zhang T, Oyama T, Horikoshi S, Hidaka H, Zhao J, Serpone N. Photocatalyzed N-demethylation and degradation of methylene blue in titania dispersions exposed to concentrated sunlight. *Sol Energy Mater Sol Cells.* 2002;73(3):287-303. doi: [10.1016/S0927-0248\(01\)00215-X](https://doi.org/10.1016/S0927-0248(01)00215-X).
  34. Sakthivel S, Neppolian B, Shankar MV, Arabindoo B, Palanichamy M, Murugesan V. Solar photocatalytic degradation of azo dye: comparison of photocatalytic efficiency of ZnO and TiO<sub>2</sub>. *Sol Energy Mater Sol Cells.* 2003;77(1):65-82. doi: [10.1016/S0927-0248\(02\)00255-6](https://doi.org/10.1016/S0927-0248(02)00255-6).
  35. Akpan UG, Hameed BH. Parameters affecting the photocatalytic degradation of dyes using TiO<sub>2</sub>-based photocatalysts: A review. *J Hazard Mater.* 2009;170(2-3):520-9. doi: [10.1016/j.jhazmat.2009.05.039](https://doi.org/10.1016/j.jhazmat.2009.05.039).
  36. Ghodbane H, Hamdaoui O. Decolorization of antraquinonic dye, CI Acid Blue 25, in aqueous solution by direct UV irradiation, UV/H<sub>2</sub>O<sub>2</sub> and UV/Fe(II) processes. *Chem Eng J.* 2010;160(1):226-31. doi: [10.1016/j.cej.2010.03.049](https://doi.org/10.1016/j.cej.2010.03.049).
  37. Talaiekhozani A, Banisharif F, Bazrafshan M, Eskandari Z, Heydari Chaleshtari A, Moghadam G, et al. Comparing the ZnO/Fe(VI), UV/ZnO and UV/Fe(VI) processes for removal of Reactive Blue 203 from aqueous solution. *Environ Health Eng Manag J.* 2019;6(1):27-39. doi: [10.15171/ehem.2019.04](https://doi.org/10.15171/ehem.2019.04).
  38. Gao BY, Yue QY, Wang Y, Zhou WZ. Color removal from dye-containing wastewater by magnesium chloride. *J Environ Manage.* 2007;82(2):167-72. doi: [10.1016/j.jenvman.2005.12.019](https://doi.org/10.1016/j.jenvman.2005.12.019).
  39. Hu Q, Liu B, Zhang z, Song M, Zhao X. Temperature effect on the photocatalytic degradation of methyl orange under UV-vis light irradiation. *Journal of Wuhan University of Technology-Mater Sci Ed.* 2010;25(2):210-3. doi: [10.1007/s11595-010-2210-5](https://doi.org/10.1007/s11595-010-2210-5).
  40. Araujo F, Yokoyama L, Teixeira L, Campos J. Heterogeneous Fenton process using the mineral hematite for the discolouration of a reactive dye solution. *Braz J Chem Eng.* 2011;28(4):605-16. doi: [10.1590/S0104-66322011000400006](https://doi.org/10.1590/S0104-66322011000400006).
  41. Barakat NAM, Kanjwal MA, Chronakis IS, Kim HY. Influence of temperature on the photodegradation process using Ag-doped TiO<sub>2</sub> nanostructures: Negative impact with the nanofibers. *J Mol Catal A Chem.* 2013;366:333-40. doi: [10.1016/j.molcata.2012.10.012](https://doi.org/10.1016/j.molcata.2012.10.012).
  42. Meric S, Kaptan D, Olmez T. Color and COD removal from wastewater containing Reactive Black 5 using Fenton's oxidation process. *Chemosphere.* 2004;54(3):435-41. doi: [10.1016/j.chemosphere.2003.08.010](https://doi.org/10.1016/j.chemosphere.2003.08.010).
  43. Benetoli LO, Cadorin BM, Postiglione CS, de Souza IG, Debacher NA. Effect of temperature on methylene blue decolorization in aqueous medium in electrical discharge plasma reactor. *J Braz Chem Soc.* 2011;22(9):1669-78. doi: [10.1590/S0103-50532011000900008](https://doi.org/10.1590/S0103-50532011000900008).
  44. Jafarnejad E, Nemati J. Methylene blue dye removal from aqueous solutions and photocatalytic activity using UV/Nano-TiO<sub>2</sub>: operating parameters study. *Anal Chem Lett.* 2015;5(4):192-7. doi: [10.1080/22297928.2015.1129289](https://doi.org/10.1080/22297928.2015.1129289).
  45. Sarvajith M, Reddy GKK, Nanchariah YV. Textile dye biodecolourization and ammonium removal over nitrite in aerobic granular sludge sequencing batch reactors. *J Hazard Mater.* 2018;342:536-43. doi: [10.1016/j.jhazmat.2017.08.064](https://doi.org/10.1016/j.jhazmat.2017.08.064).
  46. Behnajady MA, Modirshahla N, Fathi H. Kinetics of decolorization of an azo dye in UV alone and UV/H<sub>2</sub>O<sub>2</sub> processes. *J Hazard Mater.* 2006;136(3):816-21. doi: [10.1016/j.jhazmat.2006.01.017](https://doi.org/10.1016/j.jhazmat.2006.01.017).
  47. Talaiekhozani A, Salari M, Talaei MR, Bagheri M, Eskandari Z. Formaldehyde removal from wastewater and air by using UV, ferrate(VI) and UV/ferrate(VI). *J Environ Manage.* 2016;184(Pt 2):204-9. doi: [10.1016/j.jenvman.2016.09.084](https://doi.org/10.1016/j.jenvman.2016.09.084).
  48. Talaiekhozani A, Eskandari Z, Bagheri M, Talaie MR. Removal of H<sub>2</sub>S and COD using UV, ferrate and UV/ferrate from municipal wastewater. *J Hum Environ Health Promot.* 2016;2(1):1-8. doi: [10.29252/jhehp.2.1.1](https://doi.org/10.29252/jhehp.2.1.1).
  49. Koby M, Can OT, Bayramoglu M. Treatment of textile wastewaters by electrocoagulation using iron and aluminum electrodes. *J Hazard Mater.* 2003;100(1-3):163-78. doi: [10.1016/S0304-3894\(03\)00102-X](https://doi.org/10.1016/S0304-3894(03)00102-X).
  50. Talaiekhozani A, Bagheri M, Goli A, Talaie Khoozani MR. An overview of principles of odor production, emission, and control methods in wastewater collection and treatment systems. *J Environ Manage.* 2016;170:186-206. doi: [10.1016/j.jenvman.2016.01.021](https://doi.org/10.1016/j.jenvman.2016.01.021).
  51. Athar T, Hakeem A, Ahmed W. Synthesis of MgO nanopowder via non aqueous sol-gel method. *Adv Sci Lett.* 2012;7(1):27-9. doi: [10.1166/asl.2012.2190](https://doi.org/10.1166/asl.2012.2190).
  52. Vu AT, Jiang S, Ho K, Lee JB, Lee CH. Mesoporous magnesium oxide and its composites: Preparation, characterization, and removal of 2-chloroethyl ethyl sulfide. *Chem Eng J.* 2015;269:82-93. doi: [10.1016/j.cej.2015.01.089](https://doi.org/10.1016/j.cej.2015.01.089).
  53. Moussavi G, Mahmoudi M. Removal of azo and anthraquinone

- reactive dyes from industrial wastewaters using MgO nanoparticles. *J Hazard Mater.* 2009;168(2-3):806-12. doi: [10.1016/j.jhazmat.2009.02.097](https://doi.org/10.1016/j.jhazmat.2009.02.097).
54. Nematbakhsh H, Talaiekhozani A, Ahmadvand F. An Overview on Application of Nonotechnology in Environmental Engineering. Isfahan, Iran: 4th Conference of Nano-Technology from Theory to Application; 2016.
55. Yu J, Li X, Xu Z, Xiao W. NaOH-modified ceramic honeycomb with enhanced formaldehyde adsorption and removal performance. *Environ Sci Technol.* 2013;47(17):9928-33. doi: [10.1021/es4019892](https://doi.org/10.1021/es4019892).
56. Hu J, Song Z, Chen L, Yang H, Li J, Richards R. Adsorption properties of MgO (111) nanoplates for the dye pollutants from wastewater. *J Chem Eng Data.* 2010;55(9):3742-8. doi: [10.1021/je100274e](https://doi.org/10.1021/je100274e).
57. Crini G, Peindy HN. Adsorption of CI Basic Blue 9 on cyclodextrin-based material containing carboxylic groups. *Dyes Pigm.* 2006;70(3):204-11. doi: [10.1016/j.dyepig.2005.05.004](https://doi.org/10.1016/j.dyepig.2005.05.004).
58. Talaiekhozani A, Eskandari Z, Rodpeyma S, Bagheri M. Design and Development of Municipal Wastewater Treatment Systems by Fe (VI) and Computation of System's Economic Navigation. *J Adv Med Sci Appl Technol.* 2017;3(3):169-74.